

# Optimal screen arrangements for a tuned liquid damper

S. Crowley and R. Porter

(sarah.crowley@bris.ac.uk, richard.porter@bris.ac.uk)

University of Bristol, University Walk, Bristol, BS8 1TW, UK.

## 1. Introduction

Tuned Liquid Dampers (TLDs) have been installed in large engineering structures to suppress unwanted motions. They function by allowing fluid to slosh freely in a tank mounted rigidly to the structure and contain devices for dissipating energy. Here, the TLD is comprised of a two-dimensional rectangular tank and is fitted with an arbitrary number of thin vertical slatted screens through which damping can occur when the fluid is in motion.

Faltinsen et al. (2010) provide an analytic solution of the natural sloshing frequencies in a rectangular tank with a centralised slat screen. They show how these results depend on local properties of the screen such as the number and positioning of the slats. Frandsen (2005) considers the effectiveness of a TLD using a fully non-linear model. However, here the TLD is modelled as a clean tank with no screens and instead the structure is given some associated damping. Love & Tait (2010) use experimental results of structure – TLD systems to verify proposed models, with screens placed in various locations inside the tank. They conclude that a linear model is sufficient for preliminary TLD design.

To analyse the fluid motion in the tank, linearised water wave theory is adopted and a boundary-value problem developed in which homogeneous linear boundary conditions holding along the length of the screen are derived from a pair of model problems, one including an exact geometric description of a slatted screen to determine an inertia coefficient and the other using a quadratic drag law to determine an equivalent linear drag coefficient.

## 2. Formulation

We use Cartesian coordinates  $(x, y)$  with  $y = 0$  coinciding with the undisturbed free surface of a fluid contained in a two-dimensional rectangular tank with base at  $y = h$ . When at rest, the side-walls of the tank are positioned at  $x = \pm a$ , with  $N$  thin vertical slatted screens extending through the depth at  $x = a_j$ , for  $j = 1, \dots, N$ . The system

is forced into horizontal oscillations of amplitude  $\epsilon \ll a$  and with angular frequency  $\omega$ , and we are considering the long-time behaviour of the motion. The screens provide damping through the production of turbulent eddies shed from the sharp edges of the slats, and the standard arguments suggest that these eddies remain largely localised to the screen on account of the oscillating fluid motion – see Mei (1983).

On the assumption that free surface amplitudes are not excessive (this can only be checked *a posteriori*, although we note the eventual aim of this work is to suppress large oscillations with damping) we can use classical linearised water wave equations to describe the fluid motion in which the fluid velocity is given by the gradient of a potential  $\Phi(x, y, t) = \Re\{\omega\epsilon\phi(x, y)e^{-i\omega t}\}$ . Then  $\phi$  satisfies  $\nabla^2\phi = 0$  in the fluid,  $\phi_y = 0$  on  $y = h$ , and the linearised free surface condition  $K\phi + \phi_y = 0$  on  $y = 0$ , where  $K = \omega^2/g$  and  $g$  is gravitational acceleration. On the vertical walls of the tank, the horizontal velocity of the fluid is imposed by

$$\Phi_x = \omega\epsilon \cos \omega t, \quad \text{on } x = \pm a + \epsilon \sin \omega t \quad (1)$$

which, when linearised, is equivalent to requiring

$$\phi_x = 1, \quad \text{on } x = \pm a, 0 < y < h. \quad (2)$$

Finally, we require conditions relating properties of the flow from one side of a screen to the other. The horizontal velocity is continuous across the screen,

$$[\phi_x]_-^+ = 0, \quad 0 < y < h, \quad (3)$$

Where  $[\phi_x]_-^+ = \phi_x(a_j^+) - \phi_x(a_j^-)$ , for  $j = 1, \dots, N$ . A dynamic condition is also derived in the form

$$[\Phi_t(x, y, t)]_-^+ = \frac{C_D}{2}V(y, t)|V(y, t)| + LV_t(y, t) \quad (4)$$

for  $0 < y < h$  where  $V(y, t)$  is the horizontal velocity of the fluid relative to that of the screen. Here,  $C_D$  represents a drag coefficient for the screen, and  $L$  represents an inertia (or blockage) coefficient accounting for the added inertia felt by the fluid as it accelerates through the constrictions in a slatted screen, both are empirically determined. Mei

(1983) uses a local analysis of the flow field to suggest forms for  $C_D$  and  $L$ , the latter based on a long wavelength analysis.

We take a different approach, and empirically determine the drag and inertia effects from idealised mathematical models, in which the two effects of inertia and drag are isolated from one another and treated separately. We consider a simplified wave scattering problem involving a single screen at  $x = 0$  in a horizontally unbounded domain under forcing from an incident wave from  $x = -\infty$ . The approximation of an equivalent inertia coefficient  $L$  is derived by considering a perforated screen with a number of discretely defined gaps and an overall porosity of  $p$ , and thus  $kL$  is replaced by  $C$ . In contrast, the drag term is approximated through a continuous description of the screen properties, the emphasis being on developing an equivalent linear drag law from a quadratic drag law in terms of an equivalent linear drag coefficient  $\mathbb{K}_L$ .

The aim of such an approach is to derive simple, but realistic, linear relations between the pressure jump and the velocity across a screen having constant properties along its length. In accordance with (4) in which drag and inertia effects are added together, we formulate an equivalent screen boundary condition by adding together the two effects and the result is that we may transform (4) into the condition

$$[\phi]_{-}^{+} = k^{-1}\gamma(\phi_x(0, y) - 1), \quad 0 < y < h \quad (5)$$

where  $\gamma = C + i\mathbb{K}_L$  and  $k$  is defined to be the positive real root of the dispersion equation

$$K = k \tanh kh. \quad (6)$$

We consider a tank with  $N$  vertical screens placed at arbitrary positions  $x = a_j$ ,  $j = 1, \dots, N$ , shown in Fig. 1. For convenience, we extend this notation to include the two end walls by defining  $a_0 = -a$  and  $a_{N+1} = a$ .

Within each of the separate  $N + 1$  fluid-filled sections of the container, bounded by two screens  $a_j < x < a_{j+1}$ , the velocity potential is given by  $\phi = \phi^{(j)}$ , defined in terms of separation solutions as,

$$\phi^{(j)}(x, y) = \sum_{n=0}^{\infty} \chi_n^{(j)}(x) \psi_n(y), \quad (7)$$

where  $\psi_n(y)$  are vertical orthogonal eigenfunctions and  $\chi_n^{(j)}$  is given by

$$\chi_n^{(j)}(x) = \left( \frac{a_n^{(j)}}{k_n} e^{-k_n(x-a_j)} + \frac{b_n^{(j)}}{k_n} e^{k_n(x-a_j)} \right) \quad (8)$$

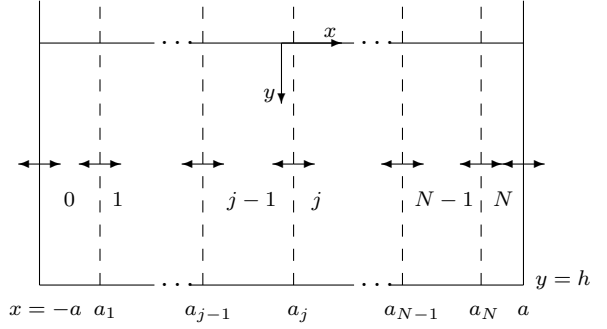


FIGURE 1:  $N$  screens inserted at  $x = a_j$ ,  $j = 1, \dots, N$  with walls at  $x = \pm a$ . The labelling indicates the  $N + 1$  separate regions of the tank.

for  $j = 0, \dots, N$ , with  $k_n$  given as the real positive roots of  $K = -k_n \tanh k_n h$  for  $n \geq 1$  and  $k_0 \equiv -ik$  where  $k$  is already defined by (6). Writing

$$1 = \sum_{n=0}^{\infty} L_n \psi_n(y) \quad (9)$$

with  $L_n = \frac{1}{h} \langle 1, \psi_n \rangle$ , denoting the inner product over  $0 < y < h$ , it is clear that the structure of the boundary conditions (2), (3) and (5) with (9) allow us to apply these conditions separately to each Fourier mode. For simplicity we will assume that each screen has the same screen properties, and then the conditions across each screen are

$$\chi_n^{(j-1)'}(a_j) = \chi_n^{(j)'}(a_j), \quad (10)$$

$$\chi_n^{(j)}(a_j) - \chi_n^{(j-1)}(a_j) = \frac{\gamma}{k} \left( \chi_n^{(j)'}(a_j) - L_n \right) \quad (11)$$

for  $j = 1, \dots, N$  and the end wall conditions are

$$\chi_n^{(0)'}(a_0) = \chi_n^{(N)'}(a_{N+1}) = L_n, \quad (12)$$

The strategy is to successively connect solutions from one section to the next through transfer matrices, before finally applying wall conditions. Such a process is reminiscent of the wide-spacing approximation widely applied to wave interactions between multiple scatterers where evanescent wave effects are often discarded to make simple connections between wave fields either side of a scatterer. Here, we are applying the same methodology but do so mode-by-mode and therefore make no approximation to the solution.

Thus, applying (11) to (8) for each  $j = 1, \dots, N$  gives

$$\begin{pmatrix} a_n^{(j-1)} \\ b_n^{(j-1)} \end{pmatrix} = T_n^{(j)} \begin{pmatrix} a_n^{(j)} \\ b_n^{(j)} \end{pmatrix} + \mu_n L_n \begin{pmatrix} e^{k_n c_j} \\ e^{-k_n c_j} \end{pmatrix} \quad (13)$$

where

$$T_n^{(j)} = \begin{pmatrix} (1 + \mu_n) e^{k_n c_j} & -\mu_n e^{k_n c_j} \\ \mu_n e^{-k_n c_j} & (1 - \mu_n) e^{-k_n c_j} \end{pmatrix} \quad (14)$$

is the transfer matrix for the  $j$ th screen,  $\mu_n = k_n \gamma / (2k)$  and  $c_j = a_j - a_{j-1}$ . Applying (14) recursively across all  $N$  screens gives

$$\begin{pmatrix} a_n^{(0)} \\ b_n^{(0)} \end{pmatrix} = \mathbf{T}_n^{(N)} \begin{pmatrix} a_n^{(N)} \\ b_n^{(N)} \end{pmatrix} + \mu_n L_n \mathbf{F}_n \begin{pmatrix} 1 \\ 1 \end{pmatrix} \quad (15)$$

where, for  $j = 1, \dots, N$ ,

$$\mathbf{T}_n^{(j)} = T_n^{(1)} T_n^{(2)} \dots T_n^{(j)} \text{ and } \mathbf{F}_n = \sum_{j=1}^N \mathbf{T}_n^{(j)}. \quad (16)$$

In deriving (15) we have made use of the fact that

$$T_n^{(j)} \begin{pmatrix} 1 \\ 1 \end{pmatrix} = \begin{pmatrix} e^{k_n c_j} \\ e^{-k_n c_j} \end{pmatrix}. \quad (17)$$

We continue by writing

$$\mathbf{T}_n^{(N)} = \begin{pmatrix} t_{11} & t_{12} \\ t_{21} & t_{22} \end{pmatrix} \text{ and } \mathbf{F}_n \begin{pmatrix} 1 \\ 1 \end{pmatrix} = \begin{pmatrix} f_1 \\ f_2 \end{pmatrix}. \quad (18)$$

Then it only remains to apply the wall conditions (12), a process which eventually gives

$$\begin{pmatrix} a_n^{(N)} \\ b_n^{(N)} \end{pmatrix} = \frac{L_n}{D} \begin{pmatrix} t_{12} - t_{22} + E e^{k_n c_{N+1}} \\ t_{21} - t_{11} + E e^{-k_n c_{N+1}} \end{pmatrix} \quad (19)$$

where  $D = (t_{21} - t_{11})e^{k_n c_{N+1}} + (t_{22} - t_{12})e^{-k_n c_{N+1}}$  and  $E = (1 - \mu_n(f_2 - f_1))$ . To recover the remaining expansion coefficients for  $j < N$ , we simply use (15) and the solution is complete.

### 3. Horizontal force on the tank

The sloshing motion of the fluid exerts hydrodynamic forces on the tank expressed as  $\Re\{F e^{-i\omega t}\}$ , and we can now find these analytically using the integrated pressure  $P = \Re\{p e^{-i\omega t}\}$ , over all vertical surfaces including the tank walls and screens. Here,  $P = -\rho \Phi_t$  so that  $p = i\omega \rho \phi$ . On account of the decomposition in (7) the depth dependence can be explicitly integrated and thus the net horizontal force for  $N$  screens is

$$F = i\omega \rho h \sum_{n=0}^{\infty} \sum_{j=0}^N L_n \left( \chi_n^{(j)}(a_j) - \chi_n^{(j)}(a_{j+1}) \right) \quad (20)$$

which, using (8) and (19) is known explicitly. It is usual practice to decompose  $F$  into its real and imaginary components by writing

$$F = -i\omega \left( A + \frac{iB}{\omega} \right), \quad (21)$$

where  $A$  is the termed the added mass and  $B$  the damping coefficient. These quantities can be non-dimensionalised using  $m = 2\rho a h$ , the mass of water in the tank, such that  $F = -i\omega m (\mu + i\nu)$  where  $A/m = \mu$  and  $B/(m\omega) = \nu$ .

### 4. Coupling tank sloshing motions to an external structure

The fluid-filled rectangular tank with damping screens investigated in the preceding sections can, when rigidly attached to a structure much larger than itself, can be used to model the effect of a so-called Tuned Liquid Damper (TLD).

The system consists of a structure of mass  $M$  which is subject to an external forcing  $F_e(t)$ , a function of time,  $t$ , and whose horizontal displacement  $X(t)$  is constrained by a linear restoring spring of stiffness  $\kappa$ . This is an idealised mechanical model of, for example, a tall building subject to wind forces. It is typical then that  $M \gg m$  where  $m$  is the mass of fluid in the attached tank and it is assumed that no external damping mechanism is attached to the mass  $M$ .

The equation of motion for the system is given by,

$$M \ddot{X}(t) = -\kappa X + F_e(t) + F_t(t), \quad (22)$$

where  $F_t(t)$  is the force exerted on the tank by the motion of the fluid within the tank.

In the absence of the tank, the undamped structure is prone to resonance at a frequency given by  $\Omega^2 = \kappa/M$ . Damping of the structural resonance can be achieved by tuning the fundamental sloshing frequency of the tank near to  $\Omega$ . This is the well-known principle by which both TLD's and tuned mass dampers (TMD's) work.

For a tank with no screens, and hence no damping, the liquid in the tank will be forced to slosh and the structural resonance at  $\Omega$  is completely suppressed, but two new resonances are introduced either side, as in Fig. 2(a). With the addition of screens the damping characteristics, the tank geometry and both the number and placement of screens, may be tuned 'optimally' such that it suppresses the structure's response to the external forcing  $F_e$ .

We assume that excitation is time-harmonic of angular frequency  $\omega$ , and then the response of the structure and the TLD will be time-harmonic also. We write  $F_{e,t}(t) = \Re\{f_{e,t} e^{-i\omega t}\}$  and  $X(t) = \Re\{x e^{-i\omega t}\}$ . The force supplied by the tank  $f_t$  is proportional to the velocity of motion ( $-i\omega x$ ). Using the non-dimensionalisation of  $A$  and  $B$  in the previous section, we rearrange the frequency-dependent equation of motion (22) to give a non-dimensional response

$$|\hat{x}| = \frac{\Omega^2/\omega^2}{|1 + \hat{m}(\mu + i\nu) - \Omega^2/\omega^2|} \quad (23)$$

where  $\hat{m} = m/M$  and  $\hat{x} \equiv x(M\Omega^2)/f_e$ .

## 5. Results

Here we use a tank of geometry  $a/h = 3$ , and let the structure have mass  $M = 10000 \text{ kg}$  and stiffness  $\kappa = 150000 \text{ N/m}$ , each per unit length of the structure. Fig. 2(a) illustrates the effectiveness of a TLD. With the addition of a screen of porosity  $p = 0.5$  in the tank, the resonant motions of the structure are effectively reduced even when, in this case, the tank is just 1.6% of the mass of the structure.

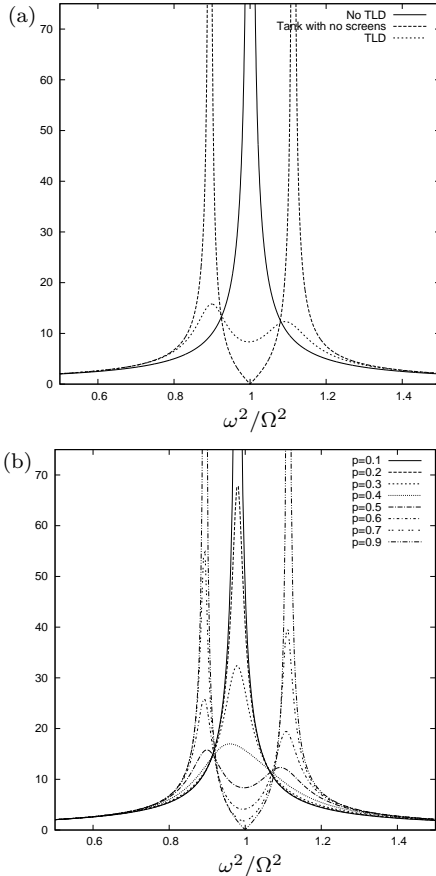


FIGURE 2: Comparison of the displacement of a structure with: (a) the addition of a tank with no screens and a TLD; (b) a TLD with a centered screen of varying porosity.

Consider Fig. 2(b), here the TLD has one centrally placed screen. If the screen is too porous the tank does not provide enough of a damping force and two resonance peaks can be seen either side of  $\omega = \Omega$ , as for a tank with no screens. If the screen is too solid,  $|\gamma| \rightarrow \infty$ , the damping becomes excessive and the sloshing fails to effectively suppress the motion of the structure at  $\omega = \Omega$ .

Consider Fig. 3, we alter both the number of placement of screens, in this example all of porosity  $p = 0.5$ . Each screen arrangement provides a different amount of damping; screens towards the outer walls of the tank providing the least, case *C*. Moving the screens towards the centre of the tank, case *B*, and then increasing the number of

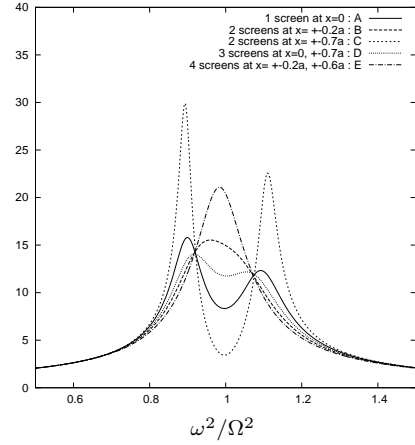


FIGURE 3: Structure displacement when coupled with a TLD with screens of porosity  $p = 0.5$  placed in various locations.

screens in the tank, case *E*, increases the inherent damping of the tank.

Notice that for screens of the same porosity all curves for varying screen locations approximately intersect at two points,  $P$  and  $Q$  say. The optimum amount of damping is attained when the peaks of the structure displacement are in the vicinity of  $P$  and  $Q$ . In TMD type systems, the intersection is exact, and this phenomenon well known. The damper is generally tuned such that the double peaks are of equal height. In the example shown in Fig. 3 it appears that the optimal configuration is case *D*.

The same process can be repeated for tanks of different geometries and screens of other porosities, such examples are to follow. Thus, in the process of designing a TLD for a particular structure, given a screen where the porosity known, the optimal arrangement and number  $N$  of these screens could be chosen in order to minimise the structural displacement when under horizontal excitation. The tank size would be determined by space limitations and liquid depth set in order to tune the sloshing frequency of the tank to the natural frequency of the structure. Alternatively, if a screen could be designed of any required porosity, for simplicity a TLD could be constructed with just one screen in the centre of the tank - with screen porosity optimised accordingly.

## 6. References

1. FALTINSEN, O.M. & TIMOKHA, A.N., 2010, *J. Sound & Vib.*, 10.1016/j.jsv.2010.10.002.
2. FRANSEN, J.B., 2005, *J. Fluids & Struct.*, **20**(3), 309–29.
3. LOVE, J.S. & TAIT, M.J., 2010, *J. Fluids & Struct.*, **26**(7–8), 1058–77.
4. MEI, C.C., 1983, *The Applied Dynamics of Ocean Surface Waves*. Wiley-Interscience.